Bacteriophage MS2 and titanium dioxide heteroaggregation: Effects of ambient light and the presence of quartz sand

Vasiliki I. Syngouna*, Constantinos V. Chrysikopoulos

School of Environmental Engineering, Technical University of Crete, 73100 Chania, Greece

A B S T R A C T

Nanoparticles (NPs) are used in numerous applications and have been observed to accumulate in natural water bodies, including aquifers where they can interact with suspended colloids and viruses. This study examines the attachment of bacteriophage MS2 onto titanium dioxide (TiO$_2$) anatase NPs using three different MS2 concentrations. Batch experiments, were conducted at room temperature to investigate the effect of ambient light and the presence of quartz sand on MS2 and TiO$_2$ NPs heteroaggregation. Appropriate attachment isotherms were determined. Extended DLVO (XDLVO) theory was used to quantify the various interaction energy profiles. The results of batch experiments demonstrated that MS2 attachment onto TiO$_2$ NPs was favored in the presence of sand under ambient light, while under dark conditions no clear trend was observed. Estimated XDLVO interaction energy profiles indicated that hydrophobic interactions may play a major role and influence the aggregation and heteroaggregation of MS2 and TiO$_2$ NPs, as well as the simultaneous attachment of MS2 and TiO$_2$ NPs onto quartz sand.

1. Introduction

Virus fate and transport, as well as virus survival in groundwater are controlled mainly by attachment onto the solid matrix and aggregation with suspended colloid particles (heteroaggregation), which could carry viruses and retain their infectivity for a long time [1–8]. The attachment, aggregation and heteroaggregation of viruses are affected by several factors including surface charge, size, environmental conditions of pH, temperature, light and relative concentration, soil chemical composition, and matrix structure [9–14].

Engineered nanoparticles (NPs) are used for the treatment of surface water, groundwater, wastewater, and other environmental systems contaminated by organic and inorganic solutes, and biocolloids (e.g. bacteria, viruses). Many studies have examined the usage of various nanomaterials as antimicrobial or antiviral agents [15–26]. Due to their ultra-small sizes, NPs may break through conventional water treatment processes and accumulate in natural water bodies [27–29]. NPs may enter various water-bodies and their interaction with aquatic pathogenic viruses is of primary consideration. Note that, due to their high surface area, NPs possess higher adsorption capacity than other equally sized colloidal particles [8,30,31].

The toxicity of TiO$_2$ NPs has been extensively investigated in the literature in order to understand the interactions between

nanomaterials and biocolloids [19,20,22,32–34]. Most of these studies were based on the photocatalytic property of TiO$_2$ NPs under UV radiation; whereas, only a handful of reports on TiO$_2$ NPs toxicity under visible light illumination and ambient light conditions are available [25,35–37]. However, it is not yet known how ambient light and the presence of quartz sand may affect the heteroaggregation of viruses and TiO$_2$ NPs.

The aim of this study was to investigate the heteroaggregation of bacteriophage MS2 and TiO$_2$ NPs at low NP concentrations (10 mg/L), in the presence of ambient light (L) and in darkness (D). Moreover, it was investigated whether the attachment of MS2 can be affected by the presence of quartz sand. Batch experiments were performed to compare the attachment of MS2 onto TiO$_2$ NPs for three different MS2 concentrations over time periods of 3 h and 7 days. Extended DLVO potential energy profiles between MS2 and TiO$_2$ NPs were constructed. In this study, MS2 bacteriophage is chosen as a surrogate microorganism for pathogenic viruses.

2. Materials and methods

2.1. Preparation and characterization of TiO$_2$ NPs

A TiO$_2$ NPs stock suspension (1000 mg/L) was prepared by

---

* Corresponding author.
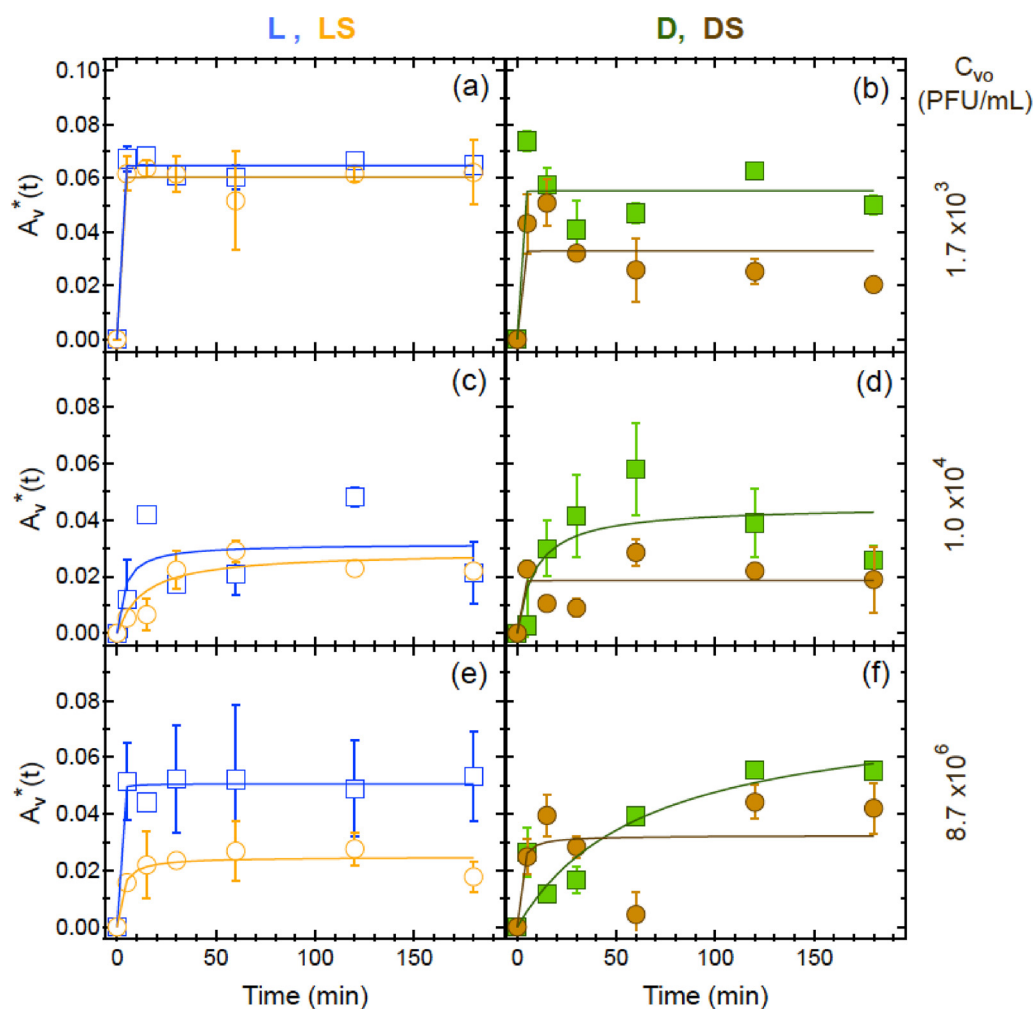   *E-mail address:* vsyngouna@isc.tuc.gr (V.I. Syngouna).

Fig. 1. Kinetics of MS2 attachment onto TiO_2 NPs under L (open squares), D (solid squares), LS (open circles) and DS (solid circles) conditions in a period of 3 h for: (a,b) $C_{v0} = 1.7 \pm 0.22 \times 10^3$ PFU/mL, (c,d) $C_{v0} = 1.0 \pm 0.14 \times 10^4$, and (e,f) $C_{v0} = 8.7 \pm 1.8 \times 10^6$ PFU/mL.

suspending TiO_2 nano-powder (anatase, > 99.9%, less than 25 nm in diameter, Sigma-Aldrich) in Milli-Q distilled deionized water (ddH$_2$O). Ti concentrations in influents and effluents of wastewater treatment plants (WWTPs) have been reported in a range of 181–1233 μg/L and < 25 μg/L, respectively [38]; as well as 3500 μg/L and 710 μg/L, respectively [39]. Effluents from WWTPs are often released in the aquatic environment. Thus, for high exposure scenarios, a homogenized and monodispersed TiO_2 suspension (10 mg/L) in a phosphate buffered saline solution (PBS) having pH 7 and ionic strength (I_s) 2 mM, was prepared for the batch experiments of this study, following the procedures reported by Syngouna and Chrysikopoulos [40]. The characteristics of TiO_2 used in this study are summarized in Table S1.

The isoelectric point (pH_{IEP}) of TiO_2 NPs in ddH$_2$O was found to be equal to 5.5, and for MS2 $pH_{IEP} = 4.1$ (see Fig. S1). The charge on TiO_2 surface changes with pH due to acid/base reactions of the surface OH group. McNamee et al. [41] reported that the pH_{IEP} for anatase TiO_2 is 5.8. The pH_{IEP} of anatase is similar to that for a single rutile TiO_2 crystal, which has been reported to occur at pH 5.6 ± 0.2 [42]. Although both rutile and anatase TiO_2 are crystalline and have an octahedron structure, they have different chemical arrangement and linkage [43,44].

2.2. Bacteriophage assay

The F-specific RNA bacteriophage, MS2 (ATCC15597-B1) with host bacterium *E. coli* (ATCC 15597), was used as a model virus because of

its comparable size, structure and behavior to that of human pathogenic viruses [45]. MS2 was assayed by the double-layer overlay method [46], as outlined by Syngouna and Chrysikopoulos [13]. The MS2 attached onto TiO_2 NPs was separated from suspended MS2 in the liquid phase by centrifugation at 2000xg for 30 min, following the procedure reported by Vasiliadou and Chrysikopoulos [47]. Because the diameter of MS2 is approximately 25 nm, whereas the TiO_2 aggregates had average diameter greater than 180 nm [40], centrifugation could efficiently settle down more than 95% of TiO_2 NPs from water [31]. The zeta potential of the MS2 was measured in PBS solution (pH = 7, $I_S = 2$ mM) by a zetasizer, and was determined to be -33.5 $\pm$ 1.8 mV [14].

2.3. Quartz sand

Quartz sand purchased directly from the manufacturer (Filcom Filterzand & Grind) with size ranging from 425 to 600 μm (sieve No 40) was used in this study. The procedure used for cleaning the quartz sand is provided in a previous publication [14]. The zeta potential of the quartz sand in PBS solution (pH = 7, $I_S = 2$ mM) was previously found to be equal to -62.25 $\pm$ 3.45 mV [14].

2.4. Batch experiments

Two sets of batch experiments were conducted in 50 mL sterilized Pyrex glass screw-cap tubes (Fisher Scientific) using PBS solution

Table 1
Fitted parameters obtained from the MS2 and TiO$_2$ kinetic attachment experiments.

Initial MS2 concentration, C_{v0} (PFU/mL)	Experimental conditions	$A^*_{v(eq)}$	k_{p2}
After 3 h			
$1.7 \pm 0.22 \times 10^3$	L	0.648	1000
	LS	0.604	900
	D	0.553	1000
	DS	0.33	1000
$1 \pm 0.14 \times 10^4$	L	0.316	0.835
	LS	0.287	0.256
	D	0.449	0.243
	DS	0.186	1000
$8.7 \pm 1.8 \times 10^6$	L	0.506	23.21
	LS	0.248	1.645
	D	0.786	0.02
	DS	0.324	2.59
After 7 days			
$1.7 \pm 0.22 \times 10^3$	L	0.506	50000
	LS	0.557	13.53
	D	0.565	799.67
	DS	0.503	7.666
$1 \pm 0.14 \times 10^4$	L	0.313	50000
	LS	0.709	0.434
	D	0.323	50000
	DS	0.447	3.420
$8.7 \pm 1.8 \times 10^6$	L	0.663	1.112
	LS	0.425	0.922
	D	0.645	1.081
	DS	0.216	3605.5

(I_S = 2 mM, pH = 7 at 25 °C) to examine the heteroaggregation of MS2 and TiO$_2$ NPs, both in the absence and presence of quartz sand, under both L and D conditions. Three initial MS2 concentrations, C_0, were chosen. The first set of experiments was conducted to examine MS2 and TiO$_2$ NPs heteroaggregation in the absence of quartz sand using two groups of glass tubes (reactor tubes, control tubes). The reactor tubes contained 50 mL of MS2 and TiO$_2$ NPs (10 mg/L) mixed suspension. Control tubes containing 50 mL of MS2 suspension without TiO$_2$ NPs were employed in order to monitor possible MS2 aggregation, time inactivation and attachment onto the tube walls. The second set of experiments was performed in the presence of quartz sand to examine both MS2 and TiO$_2$ NPs heteroaggregation, and attachment onto quartz sand. In this case, the reactor tubes contained 50 mL of MS2 and TiO$_2$ (10 mg/L) mixed suspension with 5 g of quartz sand. Control tubes containing 50 mL of MS2 suspension with 5 g of quartz sand without TiO$_2$ NPs were employed in order to monitor MS2 attachment onto both quartz sand and tube walls. Also, glass tubes containing only PBS with 5 g of quartz sand were used as blanks. Aluminum foil was used to cover the glass tubes for the experiments under dark conditions.

For both the kinetic and equilibrium attachment experiments over both of the experimental durations examined (3 h and 7 days), samples (2.0 mL) were withdrawn at different time intervals and then centrifuged to separate NPs or aggregated clusters of MS2-TiO$_2$ NPs from the freely suspended MS2 in the supernatant. The absence of TiO$_2$ NPs in the supernatant was verified by a UV–vis spectrophotometer. The concentration of the heteroaggregated MS2 and TiO$_2$ NPs was determined by mass difference. Note that for the equilibrium attachment experiments four different initial MS2 concentrations were employed.

2.5. MS2 attachment kinetics

The kinetic data from the MS2 and TiO$_2$ attachment experiments were fitted with the following pseudo-second-order model [48–50]:

$$\frac{dA^*_v(t)}{dt} = k_{p2}[A^*_{v(eq)} - A^*_v(t)]^2 \tag{1}$$

where t [min] is time; $A^*_v(t) = C^*_v(t)/C_{Total\text{-}v}(t)$ [mL/μg TiO$_2$]; $C^*_v(t)$

[PFU/μg TiO$_2$] is the concentration of MS2 attached onto TiO$_2$ NPs at time t, determined as follows:

$$C^*_v(t) = \frac{C_{Total-v}(t) - C_v(t)}{M} \tag{2}$$

where $C_{Total\text{-}v}$ [PFU/mL] is the total MS2 concentration in reactor at time t; C_v [PFU/mL] is the concentration of suspended MS2 in reactor at time t; M [μg TiO$_2$/mL] is the mass of TiO$_2$ per volume of bacteriophage suspension in the reactor; and k_{p2} [μg TiO$_2$/(mL·min)] is the rate constant of the pseudo-second order attachment. Note that $C^*_v(t)$ in Eq. 2 provides the combined concentration of infective and inactivated attached MS2 viruses. For the estimation of the pseudo-second-order model parameters the linearized form of model (1) was used [51]:

$$\frac{t}{A^*_v(t)} = \frac{1}{k_{p2}(A^*_{v(eq)})^2} + \frac{t}{A^*_{v(eq)}} \tag{3}$$

The various MS2 kinetic attachment experimental data collected in this study were fitted with the software "ColloidFit" [52]. Moreover, the percentage of MS2 attachment onto TiO$_2$ NPs at time t, P_v [%], was calculated using the following formula:

$$P_v = \frac{C_{Total\text{-}v}(t) - C_v(t)}{C_{Total\text{-}v}(t)} \times 100\% \tag{4}$$

2.6. MS2 attachment isotherms

The attachment of MS2 onto the TiO$_2$ NPs and the effect of quartz sand presence under both L and D conditions was quantified by the Freundlich isotherm, which is a non-linear relationship between MS2 concentration in the liquid phase at equilibrium, $C_{v(eq)}$ [PFU/mL], and MS2 attached concentration onto the TiO$_2$ NPs at equilibrium, $C^*_{v(eq)}$ [PFU/μg TiO$_2$], expressed as follows [53]:

$$C^*_{v(eq)} = K_f C^m_{v(eq)} \tag{5}$$

where K_f [(mL)^m/(μg TiO$_2$)(PFU)$^{m-1}$] is the Freundlich constant and m [-] is the Freundlich exponent. The Freundlich parameters K_f and m were estimated by fitting the linearized form of the Freundlich isotherm. Freundlich isotherms are essentially the superposition of many Langmuir isotherms describing sorption onto heterogeneous sorbents [54].

3. Results and discussion

3.1. Attachment kinetics of MS2 onto TiO$_2$ NPs

Fig. 1 compares the attachment kinetics of MS2 onto TiO$_2$ NPs under ambient light (L), dark (D), ambient light with the presence of quartz sand (LS) and dark with the presence of quartz sand (DS) conditions within a time period of 3 h. The MS2 kinetic experimental data (PBS solution, pH = 7 and I_S = 2 mM) were fitted with a pseudo-second-order model, and the fitted parameter values (k_{p2} and $A^*_{v(eq)}$) are listed in Table 1. The data from the kinetic batch experiments of MS2 attachment onto TiO$_2$ NPs under L and LS conditions for the three different initial MS2 concentrations were shown in Fig. 1(a,c,e). Note that for all MS2 concentrations used, higher MS2 and TiO$_2$ NPs heteroaggregation was observed under L than under LS conditions, suggesting that MS2 attachment onto TiO$_2$ NPs was hindered by the quartz sand. However, little change in the heteroaggregation of MS2 and TiO$_2$ NPs under L conditions and lower MS2 concentrations indicates that the quartz sand is controlling the aggregation process, probably by MS2 and TiO$_2$ attachment onto quartz sand, and by providing steric hindrances to attachment.

The data from the kinetic batch experiments of MS2 attachment onto TiO$_2$ NPs under D and DS conditions for the three different initial MS2 concentrations were shown in Fig. 1(b,d,f) and the fitted parameter values (k_{p2} and $A^*_{v(eq)}$) were listed in Table 1. For all MS2 initial
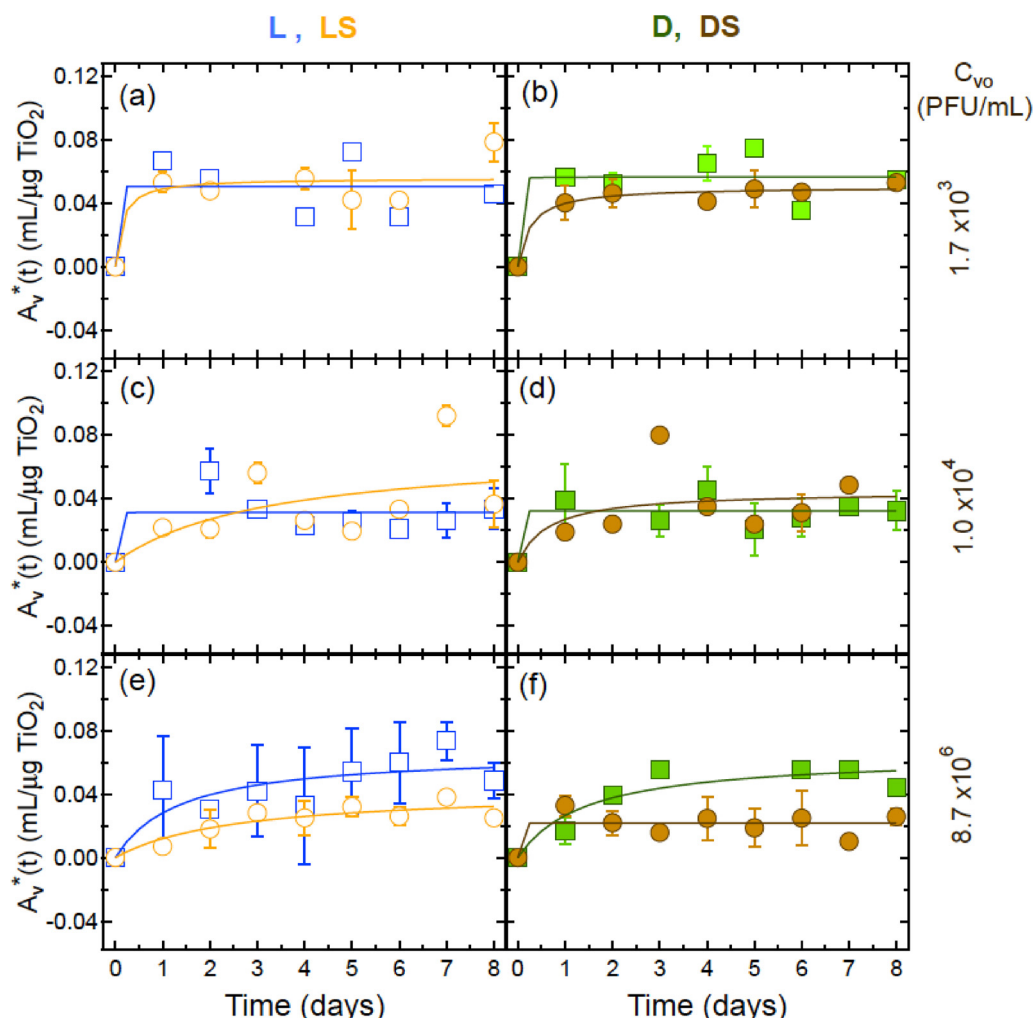
Fig. 2. Kinetics of MS2 attachment onto TiO$_2$ NPs under L (open squares), D (solid squares), LS (open circles) and DS (solid circles) conditions in a period of 7 days for: (a,b) $C_{v0} = 1.7 \pm 0.22 \times 10^3$ PFU/mL, (c,d) $C_{v0} = 1 \pm 0.14 \times 10^4$, and (e,f) $C_{v0} = 8.7 \pm 1.8 \times 10^6$ PFU/mL.

concentrations used, higher MS2 and TiO$_2$ NPs heteroaggregation was observed under D than under DS conditions. Comparison of Fig. 1(a,c,e) and 1(b,d,f) clearly suggested that for the lowest initial MS2 concentration, more MS2 was attached onto TiO$_2$ NPs under ambient light conditions (L, LS) than under dark conditions (D, DS). The opposite was observed at the highest initial concentration, while at the medium MS2 initial concentration no clear trend was observed.

Fig. 2 compares the attachment kinetics of MS2 onto TiO$_2$ NPs under L, D, LS and DS conditions within a period of 7 days. The data from the kinetic batch experiments of MS2 attachment onto TiO$_2$ NPs under L and LS conditions for the three different initial MS2 concentrations were shown in Fig. 2(a,c,e), and the fitted parameter values (k_{p2} and $A^*_{v(eq)}$) were listed in Table 1. Note that for the two lower initial MS2 concentrations, higher MS2 and TiO$_2$ NPs heteroaggregation was observed under LS than L conditions, suggesting that MS2 attachment onto TiO$_2$ NPs over the period of 7 days was facilitated by the presence of quartz sand. However, at the highest MS2 initial concentration, the opposite was observed. Under D and DS conditions (see Fig. 2(b,d,f)), at the lowest and highest initial MS2 concentrations, the presence of quartz sand hindered MS2 attachment onto TiO$_2$ NPs, while for the medium MS2 concentration the opposite was observed. Comparison of Fig. 2(a,c,e) and 2(b,d,f) clearly suggested that for all initial MS2 concentrations, similar attachment kinetics of MS2 onto TiO$_2$ NPs under L and D conditions (in the absence of quartz sand) were observed. However, in the presence of quartz sand MS2 and TiO$_2$ NPs heteroaggregation was higher under LS than DS conditions for all initial MS2

concentrations used. Furthermore, the observed differences in the heteroaggregation of MS2 and TiO$_2$ NPs for all initial concentrations under the examined conditions (L, LS, D, DS) for both time periods (see Figs. 1 and 2) do not suggest a clear trend in the MS2 aggregation process.

Fig. 3 illustrates the percent attachment of MS2 onto TiO$_2$ NPs under L, D and LS, DS experimental conditions in PBS (pH 7.0, $I_s = 2$ mM) at 25 °C over time periods of 3 h and 7 days. The greatest MS2 attachment onto TiO$_2$ NPs over both time periods tested (3 h and 7 days) was observed for the lowest MS2 initial concentration under both L and D conditions (see Table S2 and Fig. 3). The lowest MS2 attachment onto TiO$_2$ NPs was observed under DS for the medium MS2 initial concentration, over 3 h, and under LS for the highest MS2 initial concentration over 7 days (see Table S2). Although the same concentration of TiO$_2$ NPs (10 mg/L) was used for L, D, LS, and DS conditions, the attachment of MS2 onto TiO$_2$ NPs may not be compared directly, because TiO$_2$ NPs could have different primary particle sizes and aggregation states that could result in different number of available surface sites for MS2 attachment [31]. However, this study suggests higher MS2 attachment for the lowest MS2 initial concentration (see Table S2 and Fig. 3).

3.2. Isotherms of MS2 attachment onto TiO$_2$ NPs

For most of the cases examined in this study, MS2 attachment onto TiO$_2$ NPs achieved equilibrium within a few minutes (see Fig. 1). This fast equilibrium has also been observed with MS2 and FX174
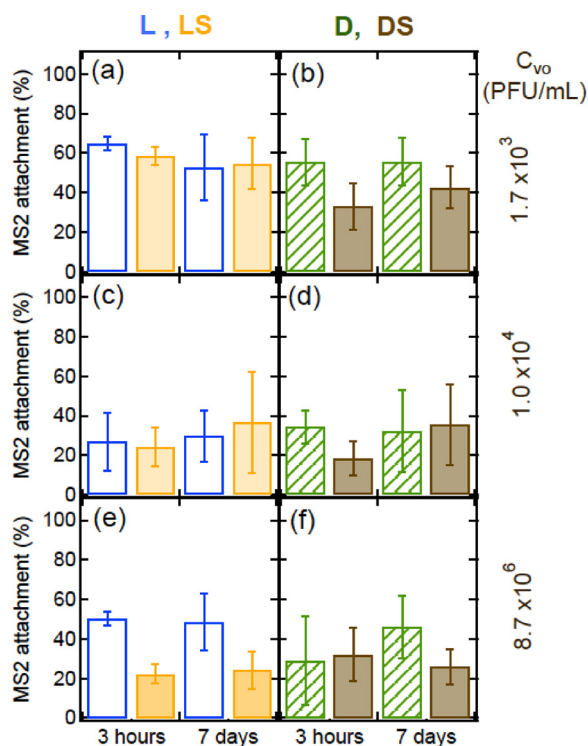
Fig. 3. Attachment percentages of MS2 onto TiO$_2$ NPs over time periods of 3 h and 7 days, under L (open columns), D (cross shaded columns) and LS, DS (filled columns) experimental conditions in PBS (pH 7.0, I$_s$ = 2 mM) at 25 °C. The first row (a,b) represents virus initial concentration of C$_{v0}$ = 1.7 ± 0.22 × 10^3 PFU/mL, the second row (c,d) C$_{v0}$ = 1 ± 0.14 × 10^4 PFU/mL, and the third row (e,f) C$_{v0}$ = 8.7 ± 1.8 × 10^6 PFU/ml.

attachment onto clay materials [5], as well as for MS2 attachment onto oxide nanoparticles [31]. Metal oxides may contribute to the removal of viruses through inactivation of attached viruses onto metal oxide surfaces [40,55,56]. Control tubes, in the absence of TiO$_2$ NPs, were used to monitor MS2 removal during the experimental period due to factors other than attachment onto TiO$_2$ NPs (e.g., inactivation or sorption onto the tube walls). However, the experimental results showed similar MS2 inactivation rates in control and reactor tubes over the experimental time period of 7 days (see Fig. S2). Note that, Syngouna and

Table 2
Freundlich isotherm parameter values for the attachment of MS2 onto TiO$_2$ NPs.

Experimental Conditions	K$_f$ [(mL)^m/(μg TiO$_2$)(PFU)$^{m-1}$]	m	R^2
L	0.099	0.99	0.99
D	0.210	0.92	0.99
LS	0.199	0.85	0.98
DS	0.086	0.91	0.99

Chrysikopoulos [40] suggested that MS2 inactivation by TiO$_2$ NPs was controlled mainly by attachment onto quartz sand and exposure to ambient light.

Fig. 4 shows equilibrium attachment data of MS2 onto TiO$_2$ NPs under L, D, LS and DS conditions. The experimental data were successfully represented with a Freundlich isotherm, and the fitted Freundlich parameters K$_f$ and m, together with the corresponding R^2 values are listed in Table 2. The greater the value of K$_f$, the higher the affinity of MS2 for TiO$_2$ NPs. Note that the Freundlich exponent m ranged from 0.85 to 1.00, suggesting that the attachment process is favorable; whereas, the R^2 values were close to 1.00, indicating that the selected Freundlich isotherm describes the adsorption process very well. The slope m is a measure of sorption intensity or surface heterogeneity, becoming more heterogeneous as its value gets closer to zero [31]. The experimental results for TiO$_2$ NPs used, under experimental conditions, clearly show that K$_f$ values increased in the presence of quartz sand under L conditions, following the trend: LS > DS and LS > L. This is attributed to the increasing surface area available for attachment in the presence of quartz sand. The compiled results listed in Table 2, indicate that, in the absence of quartz sand, the affinity of MS2 for TiO$_2$ NPs was lower under L than D conditions. This is an intuitive result because under L conditions higher MS2 inactivation occurred. Note that, viruses attached onto TiO$_2$ experienced the highest concentrations of reactive oxygen species (ROS) and inactivated more quickly than those in the bulk solution [40,57]. Sato and Taya [58] assumed that only viruses attached onto TiO$_2$ are inactivated, attachment follows the Freundlich isotherm, inactivation reaction is second-order with respect to the ROS and virus concentrations, and that active and inactive viruses have the same attachment affinity [57]. It should be noted that the hydrophilicity of TiO$_2$ NPs under UV was reported to be higher than that under visible light [59]. For that reason, it is hypothesized that a different hydrophilicity of the TiO$_2$ NP surface under
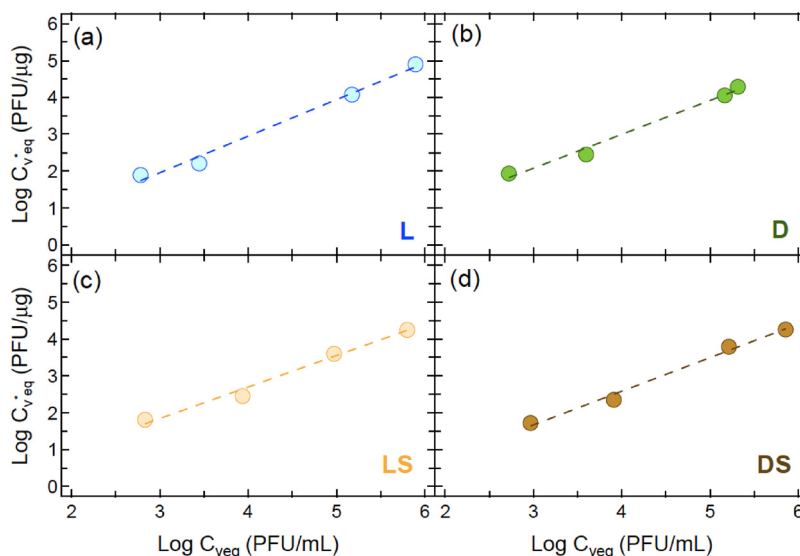

Fig. 4. Freundlich isotherms for the attachment of MS2 onto TiO$_2$ NPs under: (a) L, (b) D, (c) LS, and (d) DS experimental conditions at pH 7 and 25 °C. The corresponding Freundlich parameters K$_f$ and m are listed in Table 2.
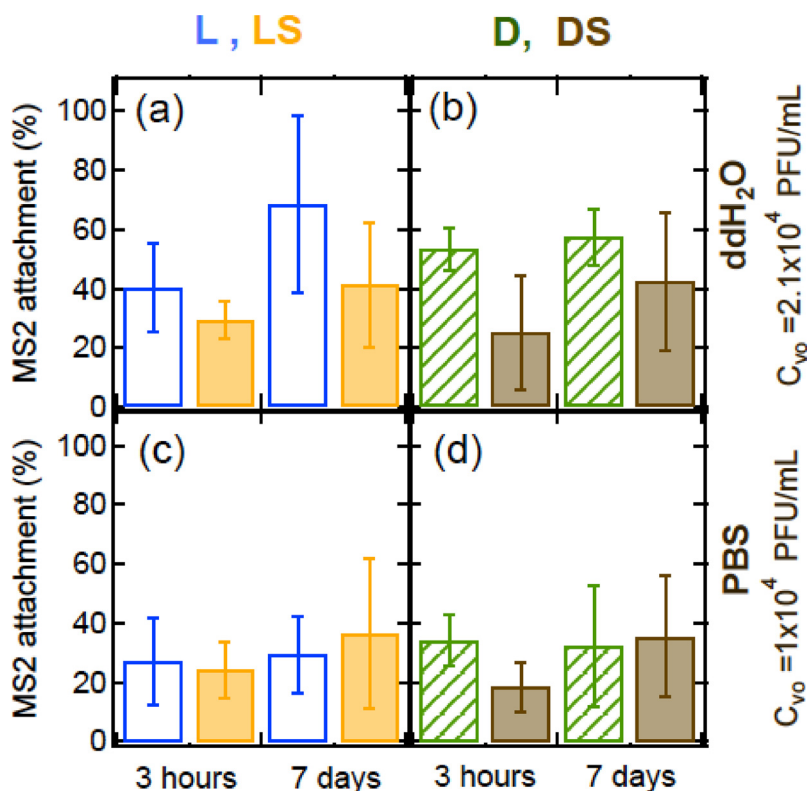
Fig. 5. Attachment of MS2 onto TiO$_2$ NPs in: (a,b) ddH$_2$O with C$_{v0}$ = 2.1 ± 0.59 × 10^4 PFU/mL, and (c,d) PBS solution with C$_{v0}$ = 1 ± 0.14 × 10^4 PFU/mL for a period of 3 h and 7 days, under L (open columns), D (cross shaded columns) and LS, DS (filled columns) experimental conditions at 25 °C.
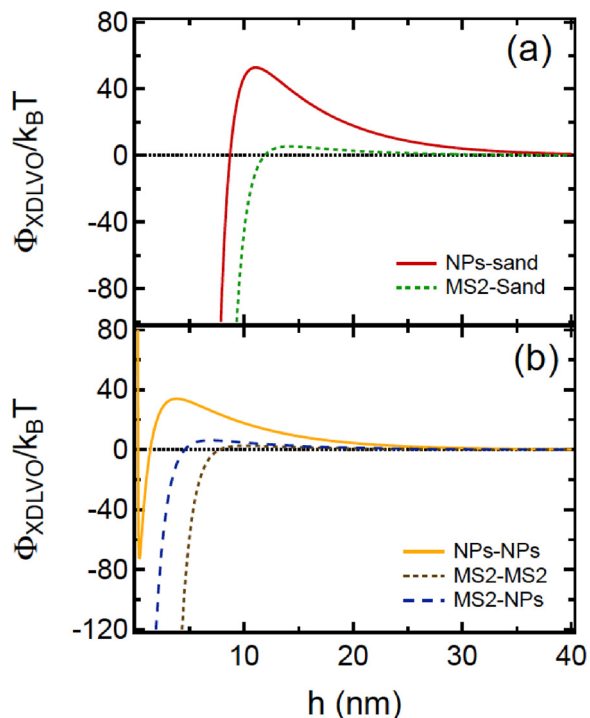

Fig. 6. Predicted XDLVO interaction energy profiles using: (a) sphere-plate approximations for MS2-Sand, and NPs-Sand, and (b) sphere-sphere for NPs-NPs, MS2-MS2, and MS2-NPs as a function of separation distance (Here PBS, pH 7, I$_s$ = 2 mM).

L and D conditions may result in different TiO$_2$ affinity towards water and different attachment behavior.

3.3. Comparison of MS2 attachment in ddH$_2$O water and PBS solution

Fig. 5 compares the MS2 attachment onto TiO$_2$ NPs in ddH$_2$O water and PBS solution for the same initial MS2 concentration to investigate the potential effect of the solution on attachment behavior of MS2. Clearly, the adsorption capacity of MS2 onto TiO$_2$ NPs in ddH$_2$O water was higher than that in the PBS solution in all cases examined in this study. The same observation was also reported by Zhang and Zhang [31] for MS2 adsorption onto various oxide NPs in ddH$_2$O water and 10 mM NaCl solution. Ionic species in PBS solution may alter the surface charges and lead to compression of the electrical double layer of both MS2 and TiO$_2$ NPs, thereby influencing electrokinetic measurements, as well as MS2 aggregation and attachment [13,60,61]. PBS solution may mask the adsorption sites of TiO$_2$ NPs and make them less available to MS2, while TiO$_2$ NPs tend to be better dispersed in ddH$_2$O and have more surface areas for MS2 adsorption [31]. Note that, MS2 coat proteins, with both negatively and positively charged moieties, could be attached onto TiO$_2$ NP surfaces through long-range electrostatic, short-range hydrophobic or specific chemical interactions with phosphate ions of PBS playing an important role in the preferential attachment process and the colloidal stability of MS2-TiO$_2$ NPs system [62]. Moreover, Syngouna and Chrysikopoulos [40] reported that MS2 inactivation by TiO$_2$ NPs was inhibited more in PBS than ddH$_2$O. Koizumi and Taya [63] found that the inactivation rate of MS2 is proportional to the MS2 mass adsorbed onto TiO$_2$.

3.4. XDLVO calculations

XDLVO theory was used to model the aggregation and heteroaggregation of MS2 and TiO$_2$ NPs and the attachment of both particles onto sand grains. Four major interfacial forces, Born (Φ_{Born}) repulsion,

van der Waals (Φ_{vdW}) attraction, electrical double layer (Φ_{dl}) repulsion, and Lewis acid-base interaction (Φ_{AB}), are considered in the calculation of surface interaction energy. In this study, TiO_2 NPs and viruses were considered spheres with diameters equal to their hydrodynamic diameters, whereas sand was regarded as an infinite plate. Interaction energy profiles for all possible MS2-NPs, MS2-MS2 and NPs-NPs, as well as, MS2-Sand, and NPs-Sand interactions were calculated using XDLVO theory for sphere-sphere and sphere-plate cases, respectively for the experimental conditions (pH = 7, I_s = 2 mM). The results are shown in Fig. 6. All calculated energy barriers (Φ_{max1}), primary minima (Φ_{min1}), and secondary minima (Φ_{min2}) are listed in Table S3. Clearly, in most cases, the Φ_{XDLVO} profiles exhibit a deep Φ_{min1}. The magnitude of Φ_{min1} depth for MS2 was found to be greater for sand than TiO_2 NPs. Similarly, greater Φ_{min1} was estimated for TiO_2 interaction with sand than with MS2. Moreover, the Φ_{max1} is lowest for MS2-MS2 interactions, and highest for TiO_2 NPs-Sand interactions (see Table S3 and Fig. 6). When TiO_2 NPs approach sand grains they face an energy barrier of 52.82 k_BT, while lower energy barriers of 5.42 k_BT and 6.26 k_BT are encountered when MS2 approaches sand and TiO_2 NPs, respectively (see Table S3 and Fig. 6). In order to evaluate the possibility of MS2 and TiO_2 aggregation, the Φ_{XDLVO} interaction energy profiles for the case of sphere-sphere approximation as applied to identical MS2-MS2 and NPs-NPs interactions were constructed under the experimental conditions (I_s = 2 mM, pH = 7) and are shown in Fig. 6b.

Worthy to note is that the Lewis acid–base free energy of interaction between two surfaces at contact, $\Phi_{AB(h=h_o)}$, was calculated based on the empirical approach by Yoon et al. [64], and was found to be more negative for MS2-Sand (-51.91 J/m^2) than TiO_2 NPs-Sand (-2.86 J/m^2) interactions and more negative for both particles with sand than MS2 interaction with TiO_2 NPs (-43.36 mJ/m^2). These findings are in perfect agreement with the experimental results of this study, showing that MS2 attachment onto TiO_2 NPs increased with the presence of quartz sand. Therefore, the XDLVO theory can successfully explain the hydrophobic interaction-mediated attachment of MS2 and TiO_2 onto sand and heteroaggregation of MS2 and TiO_2 NPs. Finally, the XDLVO theory predicts a deep primary minimum for the MS2-MS2 case, suggesting that hydrophobic interactions between MS2 particles could lead to initial aggregation (Fig. 6b).

4. Conclusions

The present study explores the interactions of MS2 with TiO_2 NPs at low exposure conditions under ambient light (L) and non-irradiated (D) conditions. The findings from this study can be employed for environmental risk assessment of these nanoparticles given their increasing usage in consumer products. The removal of viruses and other pathogens from drinking water is important for the maintenance of health and wellbeing of society. It was shown that the presence of quartz sand affects MS2 inactivation and attachment onto TiO_2 NPs under both L and D conditions. The affinity of MS2 for TiO_2 NPs increased in the presence of quartz sand under L conditions following the order LS > DS and LS > L, while under D conditions no clear trend was observed. In the absence of quartz sand, lower affinity of MS2 for TiO_2 NPs was observed under L than D conditions. The initial virus concentration can significantly affect virus attachment. Low initial virus concentrations yielded higher attachment percentage, compared to high initial virus concentrations.

Appendix A. Supplementary data

Supplementary material related to this article can be found, in the online version, at doi:https://doi.org/10.1016/j.colsurfb.2019.04.052.

References

[1] G.E. Walshe, L. Pang, M. Flury, M.E. Close, M. Flintoft, Effects of pH, ionic strength, dissolved organic matter, and flow rate on the co-transport of MS2 bacteriophages with kaolinite in gravel aquifer media, Water Res. 44 (2010) 1255–1269.

[2] V.I. Syngouna, C.V. Chrysikopoulos, Cotransport of clay colloids and viruses in water saturated porous media, Colloids Surf. A Physicochem. Eng. Asp. 416 (2013) 56–65.

[3] V.I. Syngouna, C.V. Chrysikopoulos, Experimental investigation of virus and clay particles cotransport in partially saturated columns packed with glass beads, J. Colloid Interface Sci. 440 (2015) 140–150.

[4] V.I. Syngouna, C.V. Chrysikopoulos, Cotransport of clay colloids and viruses through water-saturated vertically oriented columns packed with glass beads: gravity effects, Sci. Total Environ. 545 (2016) 210–218.

[5] C.V. Chrysikopoulos, V.I. Syngouna, Attachment of bacteriophages MS2 and ΦX174 onto kaolinite and montmorillonite: Extended-DLVO interactions, Colloids Surf. B Biointerfaces 92 (2012) 74–83, https://doi.org/10.1016/j.colsurfb.2011.11.028.

[6] V.E. Katzourakis, C.V. Chrysikopoulos, Mathematical modeling of colloid and virus cotransport in porous media: application to experimental data, Adv. Water Resour. 68 (2014) 62–73.

[7] M.I. Bellou, V.I. Syngouna, M.A. Tselepi, P.A. Kokkinos, S.C. Paparrodopoulos, A. Vantarakis, C.V. Chrysikopoulos, Interaction of human adenoviruses and coliphages with kaolinite and bentonite, Sci. Total Environ. 517 (2015) 86–95.

[8] V.I. Syngouna, C.V. Chrysikopoulos, P. Kokkinos, M.A. Tselepi, A. Vantarakis, Cotransport of human adenoviruses with clay colloids and TiO2 nanoparticles in saturated porous media: effect of flow velocity, Sci. Total Environ. 598 (2017) 159–167.

[9] C.V. Chrysikopoulos, A.F. Aravantinou, Virus attachment onto quartz sand: Role of grain size and temperature, J. Environ. Chem. Eng. 2 (2014) 796–801.

[10] G. Lipson, S.M. Stotzky, Interactions between clay minerals and viruses, Human Viruses in Sediments, Sludges, and Soils, CRC Press, Boca Raton, Florida, 1987.

[11] J.P. Loveland, J.N. Ryan, G.L. Amy, R.W. Harvey, The reversibility of virus attachment to mineral surfaces, Colloids Surf. A Physicochem. Eng. Asp. 107 (1996) 205–221.

[12] J. Zhuang, Y. Jin, Interactions between viruses and goethite during saturated flow: effects of solution pH, carbonate, and phosphate, J. Contam. Hydrol. 98 (2008) 15–21.

[13] V.I. Syngouna, C.V. Chrysikopoulos, Interaction between viruses and clays in static and dynamic batch systems, Environ. Sci. Technol. 44 (2010) 4539–4544.

[14] V.I. Syngouna, C.V. Chrysikopoulos, Transport of biocolloids in water saturated columns packed with sand: effect of grain size and pore water velocity, J. Contam. Hydrol. 129 (2012) 11–24.

[15] R.J. Watts, S. Kong, M.P. Orr, G.C. Miller, B.E. Henry, Photocatalytic inactivation of coliform bacteria and viruses in secondary wastewater effluent, Water Res. 29 (1995) 95–100.

[16] M. Cho, H. Chung, W. Choi, J. Yoon, Different inactivation behaviors of MS-2 phage and Escherichia coli in TiO2 photocatalytic disinfection, Appl. Environ. Microbiol. 71 (2005) 270–275.

[17] D. Sethi, A. Pal, R. Sakthivel, S. Pandey, T. Dash, T. Das, R. Kumar, Water disinfection through photoactive modified titania, J. Photochem. Photobiol. B Biol. 130 (2014) 310–317.

[18] A. Al-Jumaili, S. Alancherry, K. Bazaka, M.V. Jacob, Review on the antimicrobial properties of carbon nanostructures, Materials 10 (2017) 1066.

[19] A. Nel, T. Xia, L. Mädler, N. Li, Toxic potential of materials at the nanolevel, Science 311 (2006) 622–627.

[20] T.C. Long, N. Saleh, R.D. Tilton, G.V. Lowry, B. Veronesi, Titanium dioxide (P25) produces reactive oxygen species in immortalized brain microglia (BV2): implications for nanoparticle neurotoxicity, Environ. Sci. Technol. 40 (2006) 4346–4352.

[21] K. Page, R.G. Palgrave, I.P. Parkin, M. Wilson, S.L.P. Savin, A.V. Chadwick, Titania and silver-titania composite films on glass - potent antimicrobial coatings, J. Mater. Chem. (2007), https://doi.org/10.1039/b611740f.

[22] T. Xia, M. Kovochich, M. Liong, L. Mädler, B. Gilbert, H. Shi, J.I. Yeh, J.I. Zink, A.E. Nel, Comparison of the mechanism of toxicity of zinc oxide and cerium oxide nanoparticles based on dissolution and oxidative stress properties, ACS Nano 2 (2008) 2121–2134.

[23] Q. Li, S. Mahendra, D.Y. Lyon, L. Brunet, M.V. Liga, D. Li, P.J.J. Alvarez, Antimicrobial nanomaterials for water disinfection and microbial control: potential applications and implications, Water Res. 42 (2008) 4591–4602.

[24] J. You, Y. Zhang, Z. Hu, Bacteria and bacteriophage inactivation by silver and zinc oxide nanoparticles, Colloids Surf. B Biointerfaces 85 (2011) 161–167.

[25] S. Dalai, S. Pakrashi, R.S.S. Kumar, N. Chandrasekaran, A. Mukherjee, A comparative cytotoxicity study of TiO2 nanoparticles under light and dark conditions at low exposure concentrations, Toxicol. Res. (Camb.) 1 (2012) 116–130.

[26] W. Qu, S. Liu, S. Zhang, L. Wang, X. Wang, B. Sun, N. Yin, X. Gao, J.-J. Chen, et al., Graphene oxide induces toll-like receptor 4 (TLR4)-dependent necrosis in macrophages, ACS Nano 7 (2013) 5732–5745.

[27] M.A. Kiser, P. Westerhoff, T. Benn, Y. Wang, J. Perez-Rivera, K. Hristovski, Titanium nanomaterial removal and release from wastewater treatment plants, Environ. Sci. Technol. 43 (2009) 6757–6763.

[28] N. O'Brien, E. Cummins, Ranking initial environmental and human health risk resulting from environmentally relevant nanomaterials, J. Environ. Sci. Heal. Part A. 45 (2010) 992–1007.

[29] T.M. Scown, R. Van Aerle, C.R. Tyler, Do engineered nanoparticles pose a significant threat to the aquatic environment? Crit. Rev. Toxicol. 40 (2010) 653–670.

[30] W. Zhang, J. Hughes, Y. Chen, Impacts of hematite nanoparticle exposure on biomechanical, adhesive, and surface electrical properties of E. coli cells, Appl. Environ. Microbiol. (2012) AEM–00193.

[31] W. Zhang, X. Zhang, Adsorption of MS2 on oxide nanoparticles affects chlorine disinfection and solar inactivation, Water Res. 69 (2015) 59–67.

[32] M.A. Butkus, M.P. Labare, J.A. Starke, K. Moon, M. Talbot, Use of aqueous silver to enhance inactivation of coliphage MS-2 by UV disinfection, Appl. Environ. Microbiol. 70 (2004) 2848–2853.

[33] V. Ravishankar Rai, A. Jamuna Bai, A. Mendez-Vilas (Ed.), Nanoparticles and Their Potential Application as Antimicrobials, Mysore Formatex, 2011.

[34] B. Zhao, J. Zhang, Y. Jiang, Presence of bacteria in aqueous solution influences virus adsorption on nanoparticles, Environ. Sci. Pollut. Res. 20 (2013) 8245–8254.

[35] T.J. Battin, F. vd Kammer, A. Weilhartner, S. Ottofuelling, T. Hofmann, Nanostructured TiO2: transport behavior and effects on aquatic microbial communities under environmental conditions, Environ. Sci. Technol. 43 (2009) 8098–8104.

[36] I. Fenoglio, G. Greco, S. Livraghi, B. Fubini, Non-UV-induced radical reactions at the surface of TiO2 nanoparticles that may trigger toxic responses, Chem. Eur. J. 15 (2009) 4614–4621.

[37] L.V. Zhukova, J. Kiwi, V.V. Nikandrov, Nanoparticles of TiO$_2$ cause aggregation of Escherichia coli cells and suppress their division at pH 4.0-4.5 in the absence of UV irradiation, Dokl. Chem. Technol. 435 (2010) 279–282.

[38] P. Westerhoff, G.X. Song, K. Hristovski, M.A. Kiser, Occurrence and removal of titanium at full scale wastewater treatment plants: implications for TiO2 nanomaterials, J. Environ. Monit. 13 (5) (2011) 1195–1203.

[39] S.P. Bitragunta, S.G. Palani, A. Gopala, S.K. Sarkar, V.R. Kandukuri, Detection of TiO$_2$ nanoparticles in municipal sewage treatment plant and their characterization using single particle ICP-MS, Bull. Environ. Contam. Toxicol. 98 (5) (2017) 595–600.

[40] V.I. Syngouna, C.V. Chrysikopoulos, Inactivation of MS2 bacteriophage by titanium dioxide nanoparticles in the presence of quartz sand with and without ambient light, J. Colloid Interface Sci. 497 (2017) 117–125.

[41] C.E. McNamee, Y. Tsujii, M. Matsumoto, Physicochemical characterization of an anatase TiO2 surface and the adsorption of a nonionic surfactant: an atomic force microscopy study, Langmuir 21 (2005) 11283–11288.

[42] I. Larson, C.J. Drummond, D.Y.C. Chan, F. Grieser, Direct force measurements between titanium dioxide surfaces, J. Am. Chem. Soc. 115 (1993) 11885–11890.

[43] H. Cheng, J. Ma, Z. Zhao, L. Qi, Hydrothermal preparation of uniform nanosize rutile and anatase particles, Chem. Mater. 7 (1995) 663–671.

[44] D.T. Cromer, K. Herrington, The structures of anatase and rutile, J. Am. Chem. Soc. 77 (1955) 4708–4709.

[45] K. Furuse, A. Hirashima, H. Harigai, A. Ando, K. Watanabe, K. Kurosawa, Y. Inokuchi, I. Watanabe, Grouping of RNA coliphages based on analysis of the sizes of their RNAs and proteins, Virology 97 (1979) 328–341.

[46] M.H. Adams, Bacteriophages, Interscience Publishers, New York, 1959.

[47] I.A. Vasiliadou, C.V. Chrysikopoulos, Cotransport of Pseudomonas putida and kaolinite particles through water-saturated columns packed with glass beads, Water Resour. Res. 47 (2011) W02543.

[48] Y.-S. Ho, Review of second-order models for adsorption systems, J. Hazard. Mater. 136 (2006) 681–689.

[49] N.P. Sotirelis, C.V. Chrysikopoulos, Interaction between graphene oxide nanoparticles and quartz sand, Environ. Sci. Technol. 49 (2015) 13413–13421.

[50] V.I. Syngouna, G.I. Giannadakis, C.V. Chrysikopoulos, Interaction of graphene oxide nanoparticles with quartz sand in the presence of montmorillonite colloids, Environ. Technol. (2018) https://doi.org/10.1080/09593330.2018.1521876.

[51] T.V. Fountouli, C.V. Chrysikopoulos, Adsorption of pharmaceuticals, acyclovir and fluconazole, onto quartz sand under static and dynamic conditions at different temperatures, Environ. Eng. Sci. 35 (9) (2018) 909–917.

[52] V.E. Katzourakis, C.V. Chrysikopoulos, Fitting the transport and attachment of dense biocolloids in one-dimensional porous media: ColloidFit, Groundwater 55 (2017) 156–159.

[53] H.M. Freundlich, New Conception in Colloidal Chemistry, Colloid and Capillary Chemistry, Methuen Publishing Ltd, London, 1926.

[54] W.J. Weber Jr, P.M. McGinley, L.E. Katz, A distributed reactivity model for sorption by soils and sediments. 1. Conceptual basis and equilibrium assessments, Environ. Sci. Technol. 26 (1992) 1955–1962.

[55] J.N. Ryan, R.W. Harvey, D. Metge, M. Elimelech, T. Navigato, A.P. Pieper, Field and laboratory investigations of inactivation of viruses (PRD1 and MS2) attached to iron oxide-coated quartz sand, Environ. Sci. Technol. 36 (2002) 2403–2413.

[56] B. Zhao, H. Zhang, J. Zhang, Y. Jin, Virus adsorption and inactivation in soil as influenced by autochthonous microorganisms and water content, Soil Biol. Biochem. 40 (2008) 649–659.

[57] M.V. Liga, S.J. Maguire-Boyle, H.R. Jafry, A.R. Barron, Q. Li, Silica decorated TiO$_2$ for virus inactivation in drinking water–simple synthesis method and mechanisms of enhanced inactivation kinetics, Environ. Sci. Technol. 47 (2013) 6463–6470.

[58] T. Sato, M. Taya, Enhancement of phage inactivation using photocatalytic titanium dioxide particles with different crystalline structures, Biochem. Eng. J. 28 (2006) 303–308.

[59] K. Hashimoto, H. Irie, A. Fujishima, TiO$_2$ photocatalysis: a historical overview and future prospects, J. Appl. Phys. 44 (12) (2005) 8269–8285.

[60] B. Yuan, M. Pham, T.H. Nguyen, Deposition kinetics of bacteriophage MS2 on a silica surface coated with natural organic matter in a radial stagnation point flow cell, Environ. Sci. Technol. 42 (2008) 7628–7633.

[61] J. Langlet, F. Gaboriaud, J.F.L. Duval, C. Gantzer, Aggregation and surface properties of F-specific RNA phages: implication for membrane filtration processes, Water Res. 42 (2008) 2769–2777.

[62] A.E. Merryman, I.V. Sabaraya, L.S. Rowles III, A. Toteja, S.I. Carrillo, T. Sabo-Attwood, N.B. Saleh, Interaction between functionalized multiwalled carbon nanotubes and MS2 bacteriophages in water, Sci. Total Environ. 670 (2019) 1140–1145.

[63] Y. Koizumi, M. Taya, Kinetic evaluation of biocidal activity of titanium dioxide against phage MS2 considering interaction between the phage and photocatalyst particles, Biochem. Eng. J. 12 (2002) 107–116.

[64] R.-H. Yoon, D.H. Flinn, Y.I. Rabinovich, Hydrophobic interactions between dissimilar surfaces, J. Colloid Interface Sci. 185 (1997) 363–370.